The sound signature of linear viscoelastic materials

Pirouz Djoharian

THE SOUND SIGNATURE OF LINEAR VISCOELASTIC MATERIALS

Pirouz Djoharian

A.C.R.O.E.

46, av. Félix Viallet 38000 Grenoble France
Pirouz.Djoharian@imag.fr

Abstract

Frequency-damping constant relationship for normal modes of linear isotropic resonators are derived from various viscoelastic constitutive equations. As an invariant of the material, this frequency-damping relationship is then used in Physical Modeling sound synthesis, in order to represent an arbitrary shaped material.

INTRODUCTION

Vibration analysis of linear insulated resonators made of an isotropic material leads to an *invariant* relationship between frequencies and damping constants of the normal modes. The frequency-damping relationship, which we refer to as the *sound signature*, reflects the viscoelastic properties of the material. Results on the sound signature associated to common viscoelastic models will be stated. In particular, the so-called *proportional damping* assumption, known also as the Rayleigh or the modal damping [1] will be reconsidered in the light of the former results.

The knowledge of this invariant feature allows us to introduce the material as an independent parameter into Physical Modeling sound synthesis. The second part of the paper sketches a framework for Physical Modeling in terms of shape and material parameters. Thus, time domain simulation of viscoelastic resonators will be considered with emphasis on the modular synthesis approach based on discrete time rheological models.

LINEAR VISCOELASTIC BEHAVIOR

In most musical instruments, vibration of resonators is of small amplitudes. Therefore, we assume linearity throughout this work. Linear viscoelasticity considers a material sample as a linear time invariant (LTI) system with *strain* $\varepsilon(t)$ and *stress* $\sigma(t)$ as input-output pair [2]. In one dimension, the material sample is characterized by one of its response functions, for instance the step response $k_h(t)$, known as the *relaxation modulus*. The *relaxance*, which is the system transfer function is denoted as $k(s)$, where s is the Laplace variable. In three dimensions, the stress-strain relationship involves from 2 to 21 viscoelastic moduli $k_{ij}(s)$, each one having a different time/frequency dependence [2].

Relaxation spectrum

In the canonical representation, the relaxation modulus and the relaxance are expressed as

$$k_h(t) = k_e + \int_0^\infty \frac{H(\zeta)}{\zeta} e^{-\zeta t} d\zeta \qquad k(s) = k_g - \int_0^\infty \frac{H(\zeta)}{\zeta + s} d\zeta \tag{1}$$

in which $H(\zeta)/\zeta$ is the distribution of relaxation moduli and $H(\zeta)$ the relaxation *spectrum*. The constant term $k_e = k_h(\infty) = k(0)$, known as the *equilibrium* modulus is assumed positive in order to represent a viscoelastic *solid*. The *glassy* or *instantaneous* modulus $k_g = k_h(0) = k(\infty)$ is assumed finite: $k_g < \infty$. We define the non-dimensional normalized viscoelastic moduli (denoted by underlined symbols) by normalizing by k_g. For instance, $\underline{H} = H/k_g$ and $\underline{k}(s) = k(s)/k_g$.

Particular spectra

Line spectrum. A line spectrum $H(\zeta) = \Sigma k_j \delta(\zeta-\zeta_j)$ is a sum of delta functions at a finite set of relaxation frequencies. It can be represented as a combination of two idealized elements, the pure spring and the pure dashpot, in series-parallel assemblies. The two integrals in (1) reduce then to finite sums. The constitutive stress-strain relation is an ordinary differential equation. The Zener model (Fig. 1.a), with a single relaxation peak, is the simplest model of a linear viscoelastic solid. Related viscoelastic functions are

$$k_h(t) = k_e + ke^{-\zeta t} \qquad k(s) = k_g - k\frac{\zeta}{s+\zeta} \tag{2}$$

Power law spectrum. The material sample is supposed to exhibit a power law relaxation spectrum between 2 frequencies ζ_1 and ζ_2: $H(\zeta) = k_0\zeta^\theta$, with $0 \le \theta \le 1$, and $H(\zeta) = 0$ otherwise. The $\theta = 0$ case is referred to as the *box spectrum*. If, in particular $\zeta_1 = 0$ and $\zeta_2 = +\infty$, the power law spectrum leads to the Kelvin *fractional derivative* model, obtained from the Kelvin model by replacing the pure dashpot by the *spring-pot* [3]. The first integral in (1) is then converted into $k_h(t) = k_e + k_0\Gamma(\theta)t^{-\theta}$. To obtain a finite glassy modulus, the spring-pot has to be combined with pure springs in a series-parallel mounting. For example, the Zener fractional model (Fig. 1.d) has the following viscoelastic functions

$$k_h(t) = k_e + k_0\sum\frac{(-1)^n(\zeta t)^{n\theta}}{\Gamma(n\theta+1)} \qquad k(s) = k_g - k\frac{\zeta^\theta}{s^\theta+\zeta^\theta} \tag{3}$$

VISCOELASTIC OSCILLATORS

Let us consider p punctual masses interconnected by viscoelastic links represented by a transfer matrix $[K(s)]$: coefficients of $[K(s)]$ are transfer functions of the viscoelastic links. Let's say that the system is *homogeneous* if $[K(s)]$ can be factored as $[K(s)] = [K]\underline{k}(s)$, where $[K]$ is a constant matrix and $\underline{k}(s)$, a normalized relaxance, i.e. $\underline{k}(\infty) = 1$. In the modal coordinates of the conservative system defined by $[K]$ and the mass matrix $[M]$, the characteristic equation of the whole system reduces to a set of scalar equations

$$s^2 + \omega_0^2\underline{k}(s) = 0 \tag{4}$$

where ω_0 is a modal frequency of the underlying spring-mass system. Each mode can then be considered as an uncoupled scalar viscoelastic oscillator. No exact analytical solution of (4) is available, however approximate analytical forms can be obtained.

Line spectrum. If the spectrum has n delta peaks, the scalar oscillator is an $n+2$ order system having at least n negative poles $-\alpha_j$ (interlaced by the relaxation peaks $-\zeta_j$) and at most a single pair of complex oscillatory poles $-\alpha\pm i\omega$. The impulse response of the oscillator is then a sum of an oscillatory component $\exp(-\alpha\pm i\omega)t$ and a finite sum of exponential components $\exp(-\alpha_j t)$. Series expansion of (4) with respect to $(-\alpha\pm i\omega)/\zeta_{\min}$ and $\zeta_{\max}/(-\alpha\pm i\omega)$ yields the first order approximations

$$\alpha(\omega_0) \approx \sum_{j=1}^{n}\frac{\underline{k}_j}{\zeta_j}\frac{\omega_0^2}{2}, \text{ if } \omega_0 \ll \min(\zeta_j) \qquad \alpha(\omega_0) \approx \frac{1}{2}\sum_{j=1}^{n}\underline{k}_j\zeta_j, \text{ if } \omega_0 \gg \max(\zeta_j) \tag{5}$$

Free vibration of the viscoelastic oscillator is then a sum of an oscillatory component and a finite set of aperiodic components corresponding to the negative poles.

Continuous spectrum. Note that if $H(\zeta)$ possesses an analytic continuation, then $\underline{k}(s)$ has a branch cut singularity along the negative axis, running from $-\zeta_2$ to $-\zeta_1$. If $\zeta_1 > 0$, then the oscillator has a negative pole $-\alpha_1$ with $0 < \alpha_1 < \zeta_1$. The transfer function of the oscillator can then be inverted using the

integration contour shown in (Fig. 2). The impulse response of a continuous spectrum oscillator is then a combination of an aperiodic component $\exp(-\alpha_1 t)$, an oscillatory component $\exp(-\alpha \pm i\omega)t$ and a decaying function $\alpha(t)$ corresponding to the branch cut singularity

$$\alpha(t) = \mathrm{Im} \int_{\zeta_1}^{\zeta_2} \frac{e^{-st}}{s^2 + k(-s)} ds \tag{6}$$

which replaces the finite sum of decaying exponential functions in the previous case. Figure 3 shows the plot of $\alpha(t)$ in the case of a bounded power law spectrum. Note that the plot of $\alpha(t)$ is close to an exponentially decaying function. For a bounded continuous spectrum, equations (5) can be extended to the first order approximations

$$\alpha(\omega_0) \approx \frac{\omega_0^2}{2} \int_{\zeta_1}^{\zeta_2} \frac{\underline{H}(\zeta)}{\zeta^2} d\zeta \text{ , if } \omega_0 \ll \zeta_1 \qquad \alpha(\omega_0) \approx \frac{1}{2} \int_{\zeta_1}^{\zeta_2} \underline{H}(\zeta) \zeta d\zeta \text{ , if } \omega_0 \gg \zeta_2 \tag{7}$$

As a particular case, for the bounded power law spectrum, equations (7) is converted into

$$\alpha(\omega_0) \approx \omega_0^2 \frac{\underline{k}_0}{2} \frac{\zeta_2^{\theta-1} - \zeta_1^{\theta-1}}{\theta - 1} \text{, if } \omega_0 \ll \zeta_1 \qquad \alpha(\omega_0) \approx \frac{\underline{k}_0}{2} \frac{\zeta_2^{\theta+1} - \zeta_1^{\theta+1}}{\theta + 1} \text{, if } \omega_0 \gg \zeta_2 \tag{8}$$

Within the transition region $[\zeta_1, \zeta_2]$, the plot of $\alpha(\omega_0)$ in log-log axes is close to a straight line with the slope $1+\theta$ (Fig. 4).

To summarize, for a bounded spectrum, in the rubbery region, i.e. $\omega_0 \ll \zeta_1$, the damping constant is proportional to the natural frequency squared, while in the glassy region, i.e. $\omega_0 \gg \zeta_2$, the damping constant reaches a stationary value α_{max}. Note that the proportionality relation in the rubbery region, is consistent with the classical *proportional damping* assumption, often introduced in modal analysis, which assumes that the viscosity matrix is proportional to the stiffness matrix: $[Z] = \tau [K]$. In fact, for a classical second order oscillator, the last relationship induces a quadratic frequency-damping constant relationship $\alpha(\omega_0) = \tau\omega_0^2/2$, for all ω_0. Thus, proportional viscosity may reproduce approximately the $\alpha(\omega_0)$ function in the rubbery region.

In the case of the Zener fractional oscillator (see Equation 3), as $\zeta_1 = 0$, the negative pole $-\alpha_1$ disappears and the integration contour of (Fig. 2) must be adapted in order to exclude the whole negative axis. The transition frequency ζ divides the frequency axis into two regions, with two approximate forms for $\alpha(\omega_0)$:

$$\alpha(\omega_0) \approx \frac{\underline{k}}{2} \sin(\frac{\theta\pi}{2}) \frac{\omega^{\theta+1}}{\zeta^\theta} \text{, if } \omega_0 \ll \zeta \qquad \alpha(\omega_0) \approx \frac{\underline{k}}{2} \zeta^\theta \sin(\frac{\theta\pi}{2}) \omega^{1-\theta} \text{ , if } \omega_0 \gg \zeta \tag{9}$$

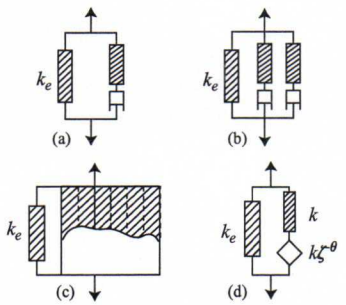

Figure 1 Viscoelastic Models: Zener (a), Wiechert model (b), Continuous Spectrum (c) and Fractional Zener (d).

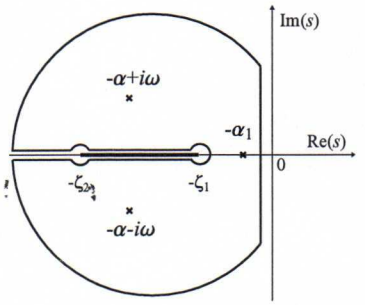

Figure 2 Integration contour for bounded spectrum oscillators.

Material sound signature

The frequency-damping constant relationships (7) and (9) are 'shape' invariant provided that $[K(s)] = [K]\underline{k}(s)$, i.e. the time and space variables are separable. By replacing the elasticity matrix $[K]$ by an

appropriate differential operator, the preceding discussion extends to simple homogeneous resonators such as strings, isotropic membranes, Euler-Bernoulli beams and isotropic Kirchhoff plates. Note that for strings, membrane and Euler-Bernoulli beams the elastic modulus k is proportional to the Young's modulus E. Thus, modal frequencies and damping constants of all of these resonators observe the same $\alpha(\omega_0)$ function, regardless of the dimensionality, the shape and the boundary conditions. However, in the case of an isotropic plate, due to the time dependence of the Poisson ratio $\nu(s)$, the *flexural rigidity* $D(s) = E(s)/(1-\nu(s)^2)$ does not have the same spectrum than the Young's modulus $E(s)$. Therefore, the $\alpha(\omega_0)$ relationship for plates is generally not identical to the one in the former cases.

In the case of anisotropic materials, or for vibration problems involving several elastic moduli, e.g. Timoshenko beams with flexural and torsional elasticity [1], the resulting frequency-damping relationship is shape dependent. In fact, in such cases, several time dependent elastic moduli combine according to the geometric data of the resonator. Therefore, no shape independent feature can be expected. It is of interest to note that, for an anisotropic resonator, the $\alpha(\omega_0)$ need not to be even an increasing function. In addition, coupled field relaxation phenomena are generally size dependent. For instance, in the case of thermoelastic relaxation, which is of great importance in metals, the relaxation peak depends on the sample width (see [2], §8.3.2).

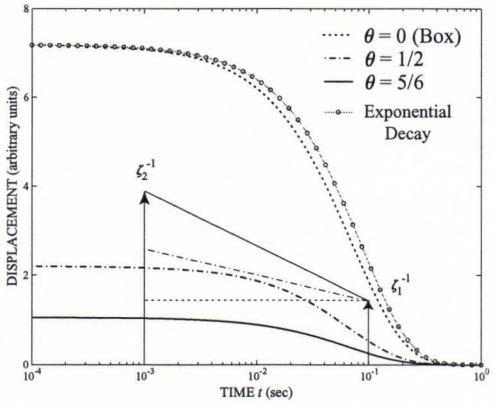

Figure 3 Plot of the $\alpha(t)$ function defined by equation (6), in the case of a bounded power law spectrum.

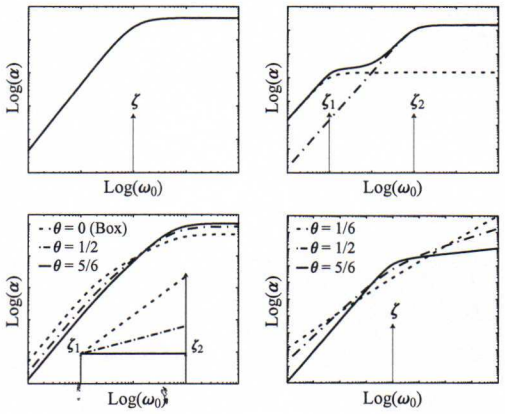

Figure 4 Damping constant vs. frequency curves corresponding to viscoelastic models represented in (Fig. 1).

PHYSICAL MODELING SOUND SYNTHESIS

The material invariant feature permits us to organize shape and material design in independent ways [4]. Shape modeling may be performed by classical approximation techniques such as finite element or finite difference methods. This way, the strain operator and geometrical data such as dimensionality and the boundary conditions are translated into the parameters of a spring-mass conservative system.

Material modeling

Given a conservative spring-mass system, defined by mass and stiffness matrices $[M]$ and $[K]$, the natural approach is to replace each pure spring with stiffness constant k_{ij} by a viscoelastic link with relaxance $k_{ij}\,\underline{k}(s)$, where $\underline{k}(s)$ is the normalized relaxance of the material. As the resulting oscillator is homogeneous in the sense defined above, it possesses a modal decomposition with real mode shapes identical to those of the underlying conservative system. However, the state space of a p degrees of freedom viscoelastic oscillator has the dimension $p(n+2)$, where n is the number of relaxation peaks. Therefore, time simulation of such high order systems is a heavy task. An alternative method is to compute a viscosity matrix $[Z]$, using the modal coordinates defined by $[K]$ and $[M]$, in order to assign to the mass-spring-dashpot system the desired $\alpha(\omega_0)$ relationship. This 'equivalent' viscous oscillator is a classical 2nd order oscillator defined by $[M]$, $[K]$ and $[Z]$. It has the same complex poles and the same mode shapes as the original $(n+2)$ order system. It should be pointed out that there is no natural way to extend the above construction to the case of a general non homogeneous viscoelastic oscillator.

In free oscillations, the missing negative poles do not have any acoustic relevance. However, in coupled situations, linear or non-linear, they can have a quite perceptible effect. For instance, consider the elementary 2-mode system of (Fig. 5), which is the (linear) elastic coupling of a unitary mass (top) with a Zener oscillator (bottom). The damping constant of the first mode of the compound system increases with the negative pole of the bottom Zener oscillator, while the converse is true for the second mode (complex poles are kept constant: α = 10 sec^{-1}, ω = 900 cps and K = 900^2 N/m). The dashed lines represent the modal damping constants if the bottom oscillator was a simple 2nd order oscillator with the same oscillatory mode. Clearly, this influence should be perceptible in non linear coupling as well. Figure 6 compares the non linear coupling of the Zener oscillator (α_1 = 1 sec^{-1}, α = 10 sec^{-1}, ω = 200 Hz) with its 'equivalent' second order oscillator (top). The spectrograms represents the responses to a square pulse of 1 second.

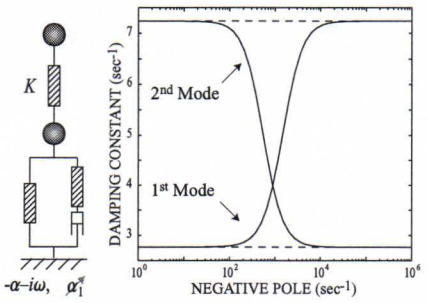

Figure 5 Influence of the negative pole on the damping constants of the (linear) coupled system

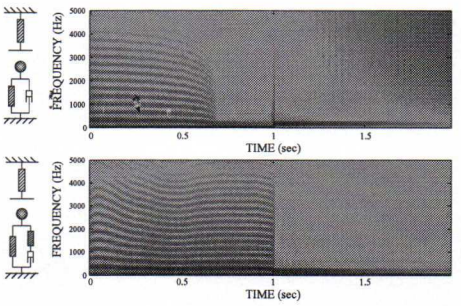

Figure 6 Step responses of the Zener oscillator (bottom) and its equivalent viscous (top), faced to a dead zone.

Discrete time rheological models

Among various methods for time discretization of finite order viscoelastic oscillators, the *modular approach* [5] is based on assembling discrete time rheological models: discrete masses, and discrete springs and dashpots. A particular advantage of this approach is the possibility to operate independent discretization schemes on the first and the second derivatives. Classical criteria are accuracy, stability and efficiency, but, due numerical dispersions, each difference scheme can be considered from the frequency-damping relationship as well.

To study the sound signature of discrete models, let us consider the Zener oscillator as a workbench. A mass m is attached to the ground by a Zener mounting defined by three parameters: the glassy modulus k_g, the relaxation peak ζ with the corresponding amplitude k. According to (4), the natural frequency ω_0 is defined by $k_g = m\omega_0^2$. By combining centered difference for the mass and respectively forward, backward and trapezoidal difference schemes for the dashpot, we obtain three 3rd order explicit schemes CF, CB and CT. The discrete Newton's 2nd law for the mass and the discrete stress-strain relationship for the dashpot are given by the following finite difference approximations

$$y_{n+1} = \frac{T_s^2}{m} f_n + -2y_n + y_{n-1} + o(T_s^2) \qquad \sigma_n = \frac{k}{\zeta}\begin{cases}(\varepsilon_{n+1} - \varepsilon_n)T_s^{-1} + o(T_s) & \text{Forward}\\ (\varepsilon_n - \varepsilon_{n-1})T_s^{-1} + o(T_s) & \text{Backward}\\ 2(\varepsilon_n - \varepsilon_{n-1})T_s^{-1} - \sigma_{n-1} + o(T_s^2) & \text{Trapeze}\end{cases} \quad (10)$$

where f and y are force and displacement and T_s the time step. It should be pointed out that combining the central difference scheme for both the mass and the dashpot leads to an unstable 4th order scheme. The same combination yields however a 2nd order accurate with acceptable stability behavior in the case of a classical 2nd order oscillator.

Stability analysis. The stability conditions of the above schemes are expressed by

$$\text{CB: } 1 + \frac{\zeta T_s}{2} - \frac{\omega_0^2 T_s^2}{4}\left(1 + (1 - \underline{k})\frac{\zeta Ts}{2}\right) > 0 \qquad \text{CF: } T_s < \frac{-\zeta + \sqrt{\zeta^2 + 4\omega_0^2 \underline{k}}}{\omega_0^2 \underline{k}} \qquad \text{CT: } Ts < \frac{2}{\omega_0} \quad (11)$$

Note that the rather complicated stability condition of CB is weaker than the CT one's: $T_s<2/\omega_0$. Thus, due to the absolute stability of the backward and the trapezoidal schemes, the corresponding stability thresholds do not depend on the viscoelastic spectrum. This is specially interesting for viscoelastic *stiff* systems involving relaxation peaks of very different magnitudes. In contrast, the stability threshold of the CF scheme, is controlled by the relaxation frequency, i.e. $T_s < 2/\zeta$ in the rubbery region, while in the glassy region, it is determined by the natural frequency: $T_s < 2/(\omega_0\sqrt{\underline{k}})$.

Dispersion analysis. Unlike continuous to discrete conversions obtained by s-plane to z-plane mappings, dispersion analysis of combined discretization schemes is rather difficult. As a general rule, centered difference for the mass raises the frequency, while the non symmetrical schemes lower it. The similar statement is true about the damping constants. However, dispersion on the damping constant is much more affected by the discretization scheme chosen for the dashpot: backward difference lowers the damping constants, while the converse is true for the forward difference. Figure 7 illustrates the relative dispersion on frequencies and damping constants. It is appropriate now to consider the resulting sound signature altered by numerical dispersions. To be consistent with the discussion on continuous time systems, the sound signature of the discrete system should be analyzed as discrete damping constants versus discrete natural frequencies. Figure 8 shows the sound signatures of the aforementioned discrete systems in comparison to the continuous one's. The CT scheme, which is of 2nd order accuracy, turns out to be the most accurate.

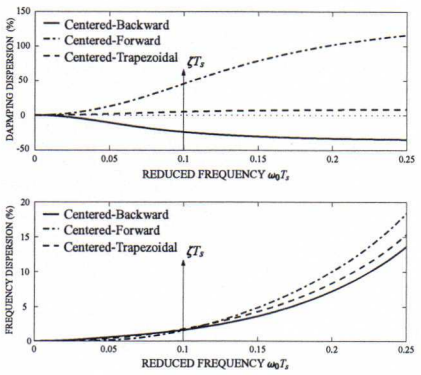

Figure 7 Numerical dispersion on damping factors and damped frequencies ($\zeta = 400$ Hz, $\underline{k} = 0.1$, $F_s = 4000$ Hz).

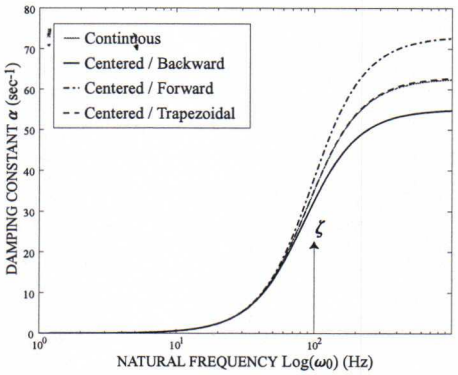

Figure 8 Signatures of the continuous and the discrete models ($F_s = 4000$ Hz, $\zeta = 100$ Hz, $\underline{k} = 0.2$).

SUMMARY

Approximate frequency-damping constant relationships for bounded spectrum and power law viscoelastic models are stated. As a shape independent feature, the frequency-damping relationship can be used as an invariant of the material in Physical Modeling sound synthesis. Discrete time rheological models are in turn analyzed in terms of the frequency-damping relation above.

REFERENCES

[1] Timoshenko, S., Young, D.H. and Weaver, W. *Vibration Problems in Engineering*. 4th edition. John Wiley & Sons, New York, 1974.

[2] Lakes, R.S. *Viscoelastic Solids*. CRC Press, Boca Raton, Florida, 1999.

[3] Koeller, R.C. "Applications of Fractional Calculus to the Theory of Viscoelasticity". *Journal of Applied Mechanics*, **51**, pp. 299-307, 1984.

[4] Djoharian, P. "Shape and Material Design in Physical Modeling Sound Synthesis", in *Proc. International Computer Music Conference*, (ICMC2000), Berlin, Germany, pp. 38-45, 2000

[5] Cadoz, C., Luciani, A. and Florens, J.L. CORDIS-ANIMA: A Modeling and Simulation System for Sound and Image Synthesis. *Computer Music Journal*, **17**, No 1, pp. 19-29, 1993.